

Tailoring heterometallic cluster functional building blocks: synthesis, separation, structural and DFT studies of [Re6-xMoxSe8(CN)6]n

V K Muravieva, y M Gayfulin, C Prestipino, P. Lemoine, M R Ryzhikov, V V Yanshole, Stéphane Cordier, Nikolay Gennadievich Naumov

▶ **To cite this version:**

V K Muravieva, y M Gayfulin, C Prestipino, P. Lemoine, M R Ryzhikov, et al.. Tailoring heterometallic cluster functional building blocks: synthesis, separation, structural and DFT studies of [Re6-xMoxSe8(CN)6]n. Chemistry - A European Journal, 2019, 25 (66), pp.15040-15045. 10.1002/chem.201903321 . hal-02280841

HAL Id: hal-02280841

https://univ-rennes.hal.science/hal-02280841

Submitted on 19 Nov 2019

HAL is a multi-disciplinary open access archive for the deposit and dissemination of scientific research documents, whether they are published or not. The documents may come from teaching and research institutions in France or abroad, or from public or private research centers.

L'archive ouverte pluridisciplinaire **HAL**, est destinée au dépôt et à la diffusion de documents scientifiques de niveau recherche, publiés ou non, émanant des établissements d'enseignement et de recherche français ou étrangers, des laboratoires publics ou privés.

10.1002/chem.201903321

WILEY-VCH

Tailoring heterometallic cluster functional building blocks: synthesis, separation, structural and DFT studies of $[Re_{6-x}Mo_xSe_8(CN)_6]^{n-}$

V.K. Muravieva,[a,b] Y.M. Gayfulin,[a] C. Prestipino,[b] P. Lemoine,[b] M.R. Ryzhikov,[a,c] V.V. Yanshole,[c,d] S. Cordier*[b] and N.G. Naumov*[a,c]

Abstract: Influence of the metal core composition and geometry on the structure, spectroscopic properties and redox potentials was investigated for the first time for heterometallic $(Re/Mo)_6$ octahedral clusters. The discrete anionic clusters $[Re_{6-x}Mo_xSe_8(CN)_6]^{n-}$ (x = 2, 3; n = 4, 5) were obtained as individual salts. Their isomeric composition and bond lengths distribution were inspected using a combination of single-crystal X-ray structure analysis, NMR, EXAFS and DFT calculations.

Octahedral cluster chalcogenides $\{M_6Q_8\}$ (M = Mo, W, Tc, Re, Q = S, Se, Te) represent an important class of inorganic compounds containing metal-metal bonds. Their structures are based on rigid M_6Q_8 core composed of the metal octahedron M_6 coordinated by the face-capped chalcogenide ligands. The M_6Q_8 moiety is additionally coordinated by apical ligands subjected to soft chemical modification. Rhenium and molybdenum clusters of this type were intensively investigated over the last decades due to the rich chemistry, structural diversity and functional properties in the solid state and in solution. Most prominent examples are: superconductivity of solid-state phases based on $[Mo_6Q_8]$ (Chevrel phases),[1] photoluminescence of discrete rhenium clusters $[Re_6Q_8L_6]^n$,[2] radiopacity,[3] and redox chemistry.[4] Numerous theoretical investigations showed that frontier molecular orbitals of the cluster core consist of the atomic orbitals of all metal atoms and (to a less extent) inner ligands.[5] Consequently, the cluster core can be considered as a chemically stable "superatom", whose composition and geometry determines the electronic structure and drives physicochemical properties of compounds.[6] Since the orbitals of each metal atom make a decisive contribution to the electronic structure of the whole cluster complex, the intrinsic properties of cluster compounds significantly depend on the nature of metals forming metallocluster.

One of the most intriguing and poorly explored possibilities that cluster complexes provide is the ability to gradually "substitute" a different number of metal atoms in a cluster core for atoms of another type, thus obtaining heterometallic cluster-based superatoms. This approach is the only practical way to investigate a gradual change in the properties of clusters at a fundamental level of structure-properties correlations during the transition from $\{M_6Q_8\}$ to $\{M'_6Q_8\}$ cores. The main difficulty of this approach is that chalcogenide clusters are synthesized by a high-temperature synthesis, and the post-synthetic modification of the octahedral metal core is unachievable without its reassembling. This feature emphasizes the importance and the need of development of experimental procedures for synthesis and separation of cluster compounds based on heterometallic cores.

The modulation of the cluster valence electron (CVE) count by a metal substitution was first applied in heterometallic Chevrel phases in 1978 with the preparation of $[Mo_2Re_4Q_8]$ (Q = S, Se) compounds.[7] The aforementioned study was then followed by the preparation and investigation of other substituted Chevrel phases: $\{Mo_{6-x}M_xQ_8\}$ (M = Re, Q = Te, x = 2; M = Ru, Q = Te, $0 \le x \le 2$, Q = Se, x = 2; M = Rh, Q = Te, x = 0.5, 1.33).[8] In contrast with polymeric phases of constant composition, the first attempt to synthesize the discrete chalcogenide clusters based on Re/Mo heterometallic cores by a high-temperature synthesis has resulted in the formation of water-soluble salts $Cs_5[Re_{6-x}Mo_xSe_8(CN)_6]\cdot nH_2O$, x = 1.64 or 1.79.[9] Our recent study has revealed that the formation of cluster cores with different ratio of metals in the melt of KCN occurs even at the optimized reaction temperature.[10]

Herein, we report the first detailed study of the discrete anionic clusters $[Re_4Mo_2Se_8(CN)_6]^{n-}$ and $[Re_3Mo_3Se_8(CN)_6]^{n-}$ as individual species. A practical method for their separation from reaction mixtures was developed. Isomerism and cluster distortion of metal cores in the solid state and in solution were investigated using a combination of single-crystal X-ray structure analysis, NMR, EXAFS and DFT calculations. In addition, spectroscopic properties and redox potentials of the heterometallic clusters were elucidated and found to be strongly correlated with the metal core composition.

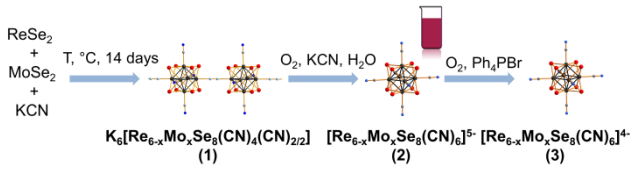
The reaction between $MoSe_2$ and $ReSe_2$ in KCN melt at high temperature results in the formation of the polymeric phase $K_6[Re_{6-x}Mo_xSe_8(\mu\text{-}CN)(CN)_4]$ with variable composition. This phase crystallizes in tetragonal space group *I4/m* and displays polymeric structure based on 1D chains composed of cluster

[a] V.K. Muravieva, Y.M. Gayfulin, M.R. Ryzhikov and N.G. Naumov
Nikolaev Institute of Inorganic Chemistry SB RAS,
630090, 3, Acad. Lavrentiev ave., Novosibirsk, Russia
E-mail: naumov@niic.nsc.ru
[b] V.K. Muravieva, C. Prestipino, P. Lemoine, S. Cordier
Univ Rennes, CNRS, ISCR (Institut des Sciences Chimiques de Rennes) UMR 6226, F-35000, France
[c] M.R. Ryzhikov, V.V. Yanshole, N.G. Naumov
Novosibirsk State University
2, Pirogova str., Novosibirsk, 630090, Russia
[d] V.V. Yanshole
International Tomography Center SB RAS
3A, Institutskaya str., Novosibirsk, 630090, Russia

Supporting information for this article is given via a link at the end of the document.

Accepted Manuscript

fragments $[Re_{6-x}Mo_xSe_8(CN)_4]$ linked by μ-CN groups in *trans*-position. It can be "depolymerized" by dissolution of the crude melt in H_2O in the presence of atmospheric O_2. This reaction is accompanied by oxidation yielding, after recrystallization, the ionic salts $K_5[Re_{6-x}Mo_xSe_8(CN)_6]\cdot nH_2O$ containing exactly the same Re/Mo ratio as initial polymer. Further metathesis reactions and recrystallization from CH_3CN in air lead to formation of salts $(Ph_4P)_4[Re_{6-x}Mo_xSe_8(CN)_6]$ according to the Scheme 1:



Scheme 1. A general way for preparation of soluble clusters from polymer phases $K_6[Re_{6-x}Mo_xSe_8(\mu\text{-}CN)(CN)_4]$ x = 2.4–3.

It was found previously that reaction at 630°C resulted in formation of the polymeric phase with x = 3.[10] Here we report that the increase of the synthesis temperature up to 800°C led to formation of isostructural polymeric phase with x varied from 2.4 to 3.0. A non-integer metal ratio in the obtained compounds indicates that these salts are composed of mixture of several discrete cluster anions, probably, $[Re_2Mo_4Se_8(CN)_6]^{n-}$, $[Re_3Mo_3Se_8(CN)_6]^{n-}$ and $[Re_4Mo_2Se_8(CN)_6]^{n-}$. To prove this assumption, several samples of the polymeric phase $K_6[Re_{6-x}Mo_xSe_8(\mu\text{-}CN)(CN)_4]$ were synthesized at different temperatures and transformed to the soluble salts with Ph_4P^+. The CH_3CN/DMF solutions of these salts were investigated using a high-resolution electrospray mass-spectrometry. It was found that the polymer prepared at 630°C yielded the salt composed of $[Re_3Mo_3Se_8(CN)_6]^{4-}$ anion with minor amount of $[Re_4Mo_2Se_8(CN)_6]^{4-}$ and $[Re_2Mo_4Se_8(CN)_6]^{4-}$ anions (Figure 1, a, Figure S4). The increase of the temperature up to 700°C and 800°C led to significant increase of the fraction of $[Re_4Mo_2Se_8(CN)_6]^{4-}$ anion (Figure 1, b, c, Figures S5, S6). It is worth noting that the $ReSe_2/MoSe_2$ ratio in the pre-loaded reaction mixture does not affect the composition of the resulting cluster phase.

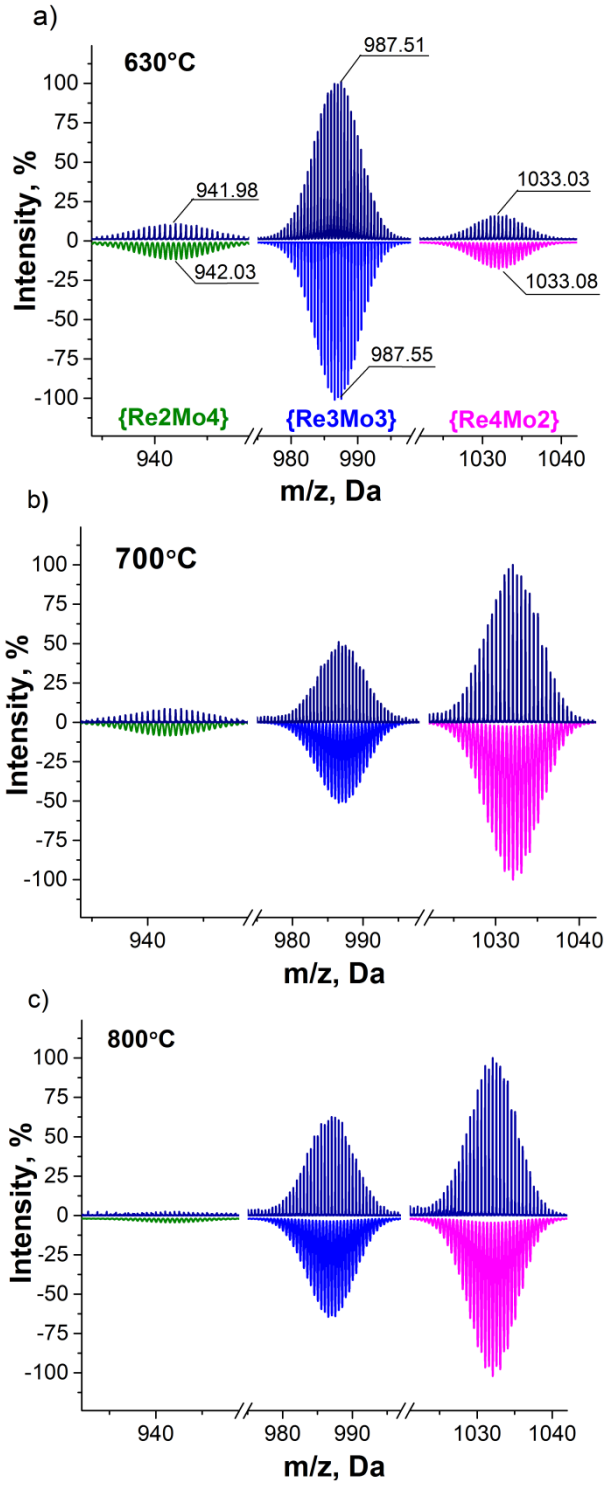


Figure 1. ESI-MS spectra in negative mode of $(Ph_4P)_4[Re_{6-x}Mo_xSe_8(CN)_6]$ salts prepared from $K_6[Re_{6-x}Mo_xSe_8(\mu\text{-}CN)(CN)_4]$ synthesized at different reaction temperatures (top) and their calculated spectra (bottom). Signals corresponds to the adducts $\{(Ph_4P)[Re_2Mo_4Se_8(CN)_6]\}^{2-}$ (m/z_{calcd} = 942.031 Da), $\{(Ph_4P)[Re_3Mo_3Se_8(CN)_6]\}^{2-}$ (m/z_{calcd} = 987.554 Da) and $\{(Ph_4P)[Re_4Mo_2Se_8(CN)_6]\}^{2-}$ (m/z_{calcd} = 1033.077 Da, left to right, correspondingly).

Accepted Manuscript

The phase $K_6[Re_{3.6}Mo_{2.4}Se_8(\mu\text{-}CN)(CN)_4]$ (**1**) synthesized at 800°C was structurally characterized (Tables S1 and S2 in Supplementary) and was used as precursor for the preparation of compounds $K_5[Re_{3.6}Mo_{2.4}Se_8(CN)_6]\cdot 11H_2O$ (**2**) and $(Ph_4P)_4[Re_{3.6}Mo_{2.4}Se_8(CN)_6]\cdot CH_3CN$ (**3**) as summarized in Scheme 1. Salts **2** and **3** contain comparable quantities of cluster anions $[Re_4Mo_2Se_8(CN)_6]^{n-}$ and $[Re_3Mo_3Se_8(CN)_6]^{n-}$.

We have found an easy and convenient method of separation of cluster anions $[Re_3Mo_3Se_8(CN)_6]^{5-}$ and $[Re_4Mo_2Se_8(CN)_6]^{5-}$ based on the difference of redox properties of these clusters. A crucial stage in the separation procedure is the addition of aqueous solution of *n*-Bu_4NBr to the aqueous solution of **2** during stirring in air. Anion $[Re_4Mo_2Se_8(CN)_6]^{5-}$ was found to be unstable toward oxidation in these conditions and this led to the precipitation of the salt $(n\text{-}Bu_4N)_4[Re_4Mo_2Se_8(CN)_6]$ (**4**) as individual phase containing the anion $[Re_4Mo_2Se_8(CN)_6]^{4-}$ (22 CVE) only. The remaining colored mother solution contains the $[Re_3Mo_3Se_8(CN)_6]^{5-}$ anion, and further precipitation was not observed even after long exposure of the solution in air or addition of large excess of *n*-Bu_4NBr. The extraction of $[Re_3Mo_3Se_8(CN)_6]^{5-}$ from aqueous solution by CH_2Cl_2 was successful. Crystallization of the highly charged anion $[Re_3Mo_3Se_8(CN)_6]^{5-}$ in organic solution was not achieved. One electron oxidation of $[Re_3Mo_3Se_8(CN)_6]^{5-}$ was performed in order to reduce the charge of the cluster anion (Figure 2). Then diffusion of Et_2O vapor into solution with oxidized cluster led to formation of crystalline salt $(n\text{-}Bu_4N)_4[Re_3Mo_3Se_8(CN)_6]$ (**5**) containing the anion $[Re_3Mo_3Se_8(CN)_6]^{4-}$ (21 CVE). Mass-spectrometry investigations confirm the selectivity of separation. The mass spectra of **5** in CH_2Cl_2 demonstrates the presence of $[Re_3Mo_3Se_8(CN)_6]^{n-}$ anion adducts only (Figure S8). The ESI-MS spectra of **4** in acetone demonstrates the signals for adducts of $[Re_4Mo_2Se_8(CN)_6]^{4-}$ without noticeable admixtures of $[Re_3Mo_3Se_8(CN)_6]^{4-}$ (Figure S7). $[Re_3Mo_3Se_8(CN)_6]^{5-}$ anion can be also isolated from organic media as water soluble salt $K_5[Re_3Mo_3Se_8(CN)_6]\cdot 11H_2O$ (**6**) by means of metathesis reaction with KSCN.

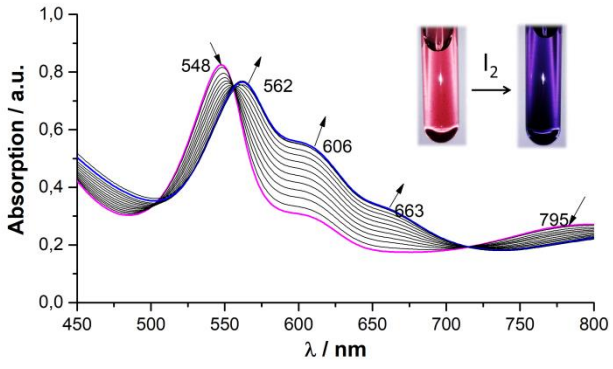


Figure 2. Evolution of UV-Vis spectra of $[Re_3Mo_3Se_8(CN)_6]^{5-/4-}$ anions (compound **5**) in DMF solution during redox titration by iodine solution. Purple line corresponds to the $[Re_3Mo_3Se_8(CN)_6]^{5-}$ anion, blue line – to the $[Re_3Mo_3Se_8(CN)_6]^{4-}$ one.

One can see that the selective one-electron oxidation of $[Re_4Mo_2Se_8(CN)_6]^{5-}$ anion by air oxygen and the formation of insoluble salt **4** in water are the driving forces of the separation process. Examination of redox properties of $[Re_4Mo_2Se_8(CN)_6]^{4-}$ anion in electrochemical conditions displayed two quasi-reversible redox waves characterized by $E_{1/2}$ values of –0.476 V and –1.294 V *vs* Ag/AgCl (Figure 3, Table 1). These processes correspond to the reduction of $[Re_4Mo_2Se_8(CN)_6]^{4-}$ cluster with 22 CVE and consequent formation of $[Re_4Mo_2Se_8(CN)_6]^{5-}$ anion with 23 CVE and $[Re_4Mo_2Se_8(CN)_6]^{6-}$ anion with 24 CVE, respectively. CV curve of $[Re_3Mo_3Se_8(CN)_6]^{5-}$ anion (compound **5** in CH_3CN, Figure S10) showed three successive steps of reduction forming $[Re_3Mo_3Se_8(CN)_6]^{5-/6-/7-}$ anions (22, 23 and 24 CVE, respectively). Half-wave potentials of these processes in CH_3CN were -0.202 V, -0.870 V and -1.270 V, respectively. It is important to note that the increase of Mo content within the cluster core causes significant negative shift of potential corresponding to oxidation process from 24 to 23 CVE and to the appearance of further oxidation from 23 to 22 and from 22 to 21 CVE redox pairs (Table 1). Therefore, a non-isovalent substitution of metal atoms in the cluster core is a powerful tool for tuning of the redox properties of cluster compounds. The difference of electrochemical potentials of $[Re_3Mo_3Se_8(CN)_6]^{5-}$ and $[Re_4Mo_2Se_8(CN)_6]^{5-}$ anions (Table 1) allowed the selective oxidation of the latter. Complete oxidation of $[Re_4Mo_2Se_8(CN)_6]^{5-}$ anion and precipitation of **4** occur at pH 7-9, while $[Re_3Mo_3Se_8(CN)_6]^{5-}$ anion remains in solution.

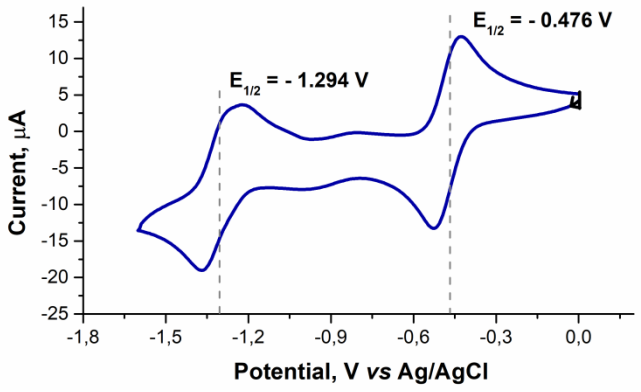


Figure 3. Cyclic voltammogram of **4** in CH_3CN under Ar, 25 $mV\cdot sec^{-1}$ scan rate.

Table 1. Redox data for $\{M_6Se_8\}$-type clusters (M = Re, Mo; potentials are normalized *vs* Ag/AgCl/3.5 M KCl electrode). Redox pair charges are in brackets.

Anion	20/21	21/22	22/23	23/24
$[Re_6Se_8(CN)_6]$ (CH_3CN)[4]	–	–	–	0.125 (3-/4-)
$[Re_4Mo_2Se_8(CN)_6]$ (CH_3CN)	–	–	-0.476 (4-/5-)	-1.294 (5-/6-)

Accepted Manuscript

$[Re_3Mo_3Se_8(CN)_6]$ (CH_3CN)	–	-0.202 (4-/5-)	-0.870 (5-/6-)	-1.270 (6-/7-)
$[Re_3Mo_3Se_8(CN)_6]$ (DMF)[10]	–	-0.325 (4-/5-)	-0.818 (E_{pc}) (5-/6-)	-1.410 (6-/7-)
$[Mo_6Se_8(CN)_6]$ (H_2O)[11]	-0.647 (6-/7-)	-1.081 (7-/8-)	-1.574 (8-/9-)	–

It is obvious, that $\{Re_3Mo_3Se_8\}$ and $\{Re_4Mo_2Se_8\}$ cores can also exist in two isomeric forms each (Figure 4). According to our crystallographic data, high symmetry of the lattice results in shared occupancy of Re and Mo atoms in metal sites, that does not allow to distinguish these forms due to their co-crystallization and orientational disorder. In order to shed light on the isomeric composition of obtained clusters, ^{77}Se NMR spectra of diamagnetic 22 CVE cluster salts **4** and **6** were recorded in acetone and H_2O, respectively.

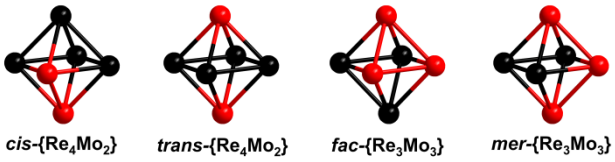


Figure 4. Isomerism of the octahedral metal cores $\{Re_3Mo_3\}$ and $\{Re_4Mo_2\}$.

The $\{Re_3Mo_3Se_8\}$ cluster can exists as *mer*-$\{Re_3Mo_3Se_8\}$ isomer of C_{2v} symmetry comprising two types of chemically non-equivalent selenium atoms in the ratio of 4:4, or *fac*-$\{Re_3Mo_3Se_8\}$ of C_{3v} symmetry exhibiting four non-equivalent selenium atoms in the ratio of 1:3:3:1. The ^{77}Se NMR spectrum of **6** contains two signals at 172 and 365 ppm with close integral intensities (Figure 5a). This finding should be attributed to the existence of *mer*-$\{Re_3Mo_3Se_8\}$ isomer only.

Similar consideration of the $\{Re_4Mo_2Se_8\}$ isomers leads to three different types of selenium atoms giving NMR signals with 2:4:2 theoretical intensities for *cis*-$\{Re_4Mo_2Se_8\}$ isomer and only one signal for *trans*-$\{Re_4Mo_2Se_8\}$ isomer. ^{77}Se NMR spectrum of **4** demonstrated four signals at 14, 297, 322 and 495 ppm (Figure 5b) indicating the mixture of both *cis*- and *trans*- isomers. The content of *cis*-$\{Re_4Mo_2Se_8\}$ was estimated as about twice higher than *trans*-$\{Re_4Mo_2Se_8\}$. The results of NMR spectroscopy demonstrated that high temperature synthesis likely lead to the formation of only *mer*-isomer in case of $\{Re_3Mo_3Se_8\}$ and both *cis*- and *trans*- isomers in case of $\{Re_4Mo_2Se_8\}$ cluster, with 1:2 ratio in the polymeric phase $K_6[Re_{3.6}Mo_{2.4}Se_8(\mu\text{-}CN)(CN)_4]$ (**1**) and products of its metathesis.

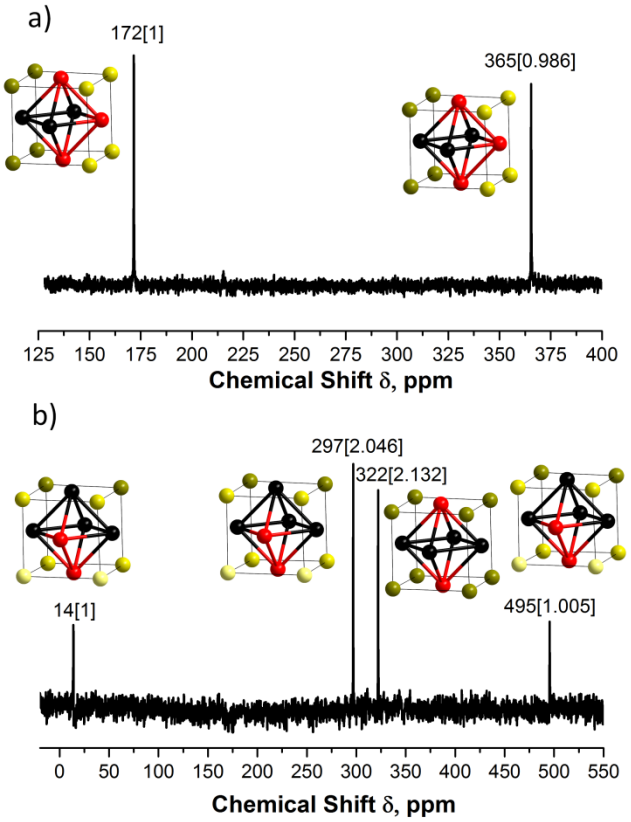


Figure 5. ^{77}Se NMR spectra for a) **6** in D_2O b) **4** in CD_3COCD_3, integrated intensities are shown in brackets.

To analyze the optimized geometry and electronic structure of novel heterometallic–cores $\{Re_4Mo_2\}$, DFT calculations were performed for both *cis*- and *trans*- isomers of $[Re_4Mo_2Se_8(CN)_6]^{n-}$ anion (n = 4–6, CVE count from 22 to 24). Molecular orbital (MO) diagrams for $[Re_4Mo_2Se_8(CN)_6]^{n-}$ isomers are shown in Figure 6. Orbitals of 24 CVE clusters have mixed bonding-antibonding character relative to metal-metal interactions below Fermi energy level (HOMO, HOMO-1 and etc.) and anti-bonding above the Fermi energy level (LUMO, LUMO+1 and etc.). The HOMO and HOMO-1 are composed mostly of rhenium and molybdenum atomic orbitals with some contribution of selenium atomic orbitals (about 25%). The MO disposition demonstrates the presence of relatively large HOMO-LUMO gap of ~2 eV and smaller gap of 0.6-0.7 eV between HOMO-1 and HOMO-2 (for 23 and 24 CVE cluster anions).

Accepted Manuscript

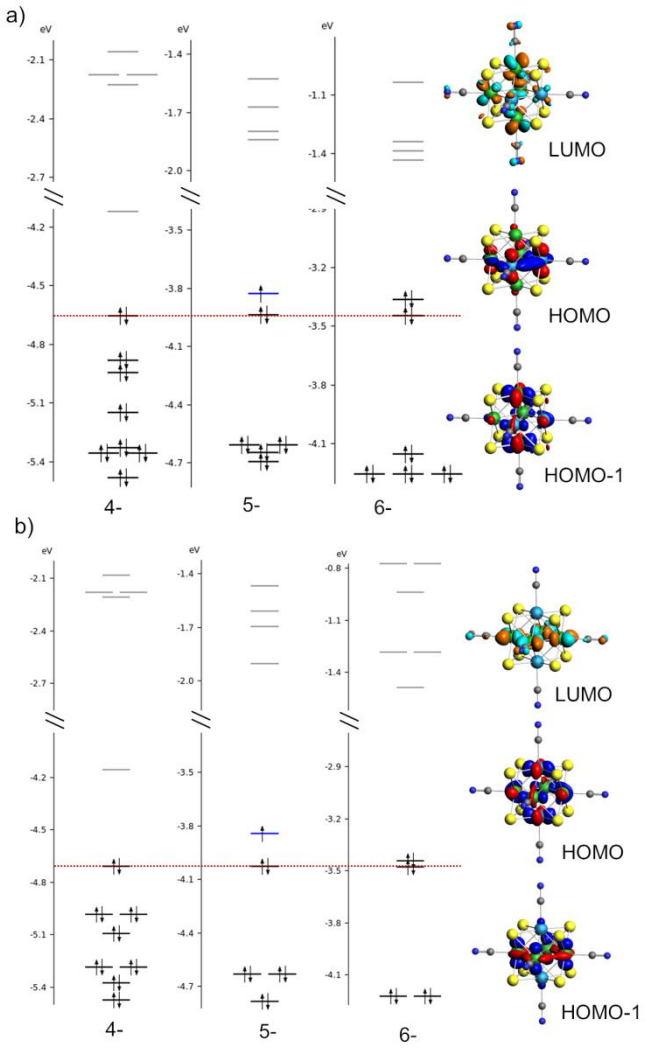


Figure 6. Molecular orbital diagrams of *cis*- (a) and *trans*- (b) isomers of $[Re_4Mo_2Se_8(CN)_6]^{n-}$ (n = 4–6 from left to right). On the insets: typical view of the HOMO-1, HOMO and LUMO for $[Re_4Mo_2Se_8(CN)_6]^{5-}$ anion. The diagrams are lined on the HOMO-1 level.

The calculated mean M–M distances for isomers of $[Re_4Mo_2Se_8(CN)_6]^{4-}$ anion are listed in Table 2. The attentive analysis of optimized geometries reveals that both *cis*- and *trans*-isomers of 24 CVE $\{Re_4Mo_2\}$ cores are barely distorted, with close metal-metal distances. Removal of two valence electrons from HOMO level causes strong distortion of metal cores in both *cis*- and *trans*- isomers (Figure 7a). The octahedral distortion leads to the loss of the O_h symmetry by axial distortion to D_{4h}-symmetrized *trans*-isomer. Elongation of the metal bond in the case of *cis*-$[Re_4Mo_2Se_8(CN)_6]^{4-}$ anion leads to C_{2V} point symmetry (Figure 7b). The difference between the shortest and the largest M-M bonds of 22-electron $[Re_4Mo_2Se_8(CN)_6]^{4-}$ anion has the remarkable values of 0.197 and 0.091 Å for *cis*- and *trans*-isomer, respectively. In both cases the distortion is provided by the preference of molybdenum to form longer and rhenium – shorter distances with the surrounding atoms (Table 2). Mo-Se and Re-Se distances are close and do not show the similar consistency as metal distances (Table S5). It is worth noting that average M–M bond distances are practically equal for both isomers and all CVE counts (Figure 7a), and are close to the data of single-crystal X-Ray structural analysis.

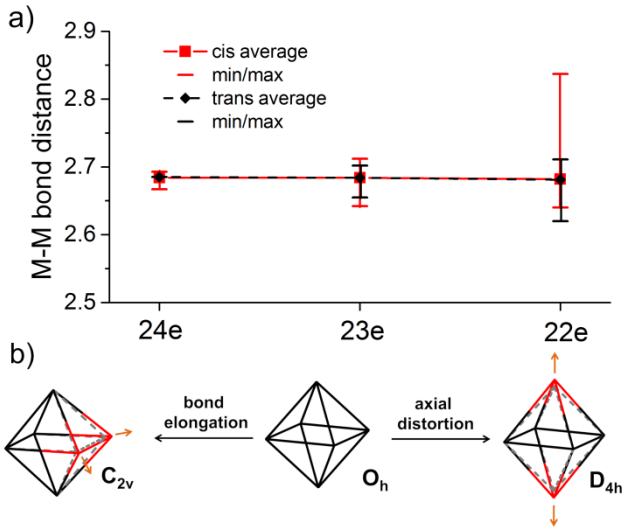


Figure 7. a) analysis of the DFT optimized geometries of the anions $[Re_4Mo_2Se_8(CN)_6]^{n-}$ n = 6-(24 electrons), 5- (23e$^-$), 4- (22e$^-$) b) octahedral distortion in 22-electron $\{Re_4Mo_2\}$ metal cores.

Table 2. The comparison of the M–M distances and octahedron diagonals (R_d) for 22-electron $\{Re_4Mo_2\}$ metal core obtained by theoretical and experimental techniques.

	cis-$\{Re_4Mo_2\}$		*trans*-$\{Re_4Mo_2\}$		SC XRD
	EXAFS model	DFT model	EXAFS model	DFT model	
$R_{Mo\text{-}Mo}$	2.784	2.837	–	–	–
$R_{Mo\text{-}Re}$	2.678	<2.685>	2.671	<2.711>	–
$R_{Re\text{-}Re}$	2.629	<2.648>	2.636	<2.620>	–
$R_{M\text{-}M}$	<2.667>	<2.682>	<2.659>	<2.681>	<2.646(14)>

To evaluate the real geometry of $\{Re_4Mo_2\}$ and $\{Re_3Mo_3\}$ cluster cores, Extended X-Ray Absorption Fine Structure (EXAFS) measurements were carried out on Mo K-edge and Re L_3-edge for solids $(n\text{-}Bu_4N)_4[Re_4Mo_2Se_8(CN)_6]$ (**4**) and $K_5[Re_3Mo_3Se_8(CN)_6]\cdot 11H_2O$ (**6**) both having 22 CVE, which have the most significant distortion of metal core according to DFT calculations. The experimental data obtained for Re and Mo have been simultaneously fitted by the model containing pure isomeric atom arrangement. The final theoretical functions for both isomers in the case of $\{Re_4Mo_2\}$ agree well with the experimental spectra (Figure 8, Figure S12). The final fitting parameters can

Accepted Manuscript

be found in Table S3. The resulted metal-metal distances obtained by the fitting of the EXAFS spectra and respective octahedron distortion were found to follow the same trend as DFT optimized geometries (Table 2). Both fits revealed visibly enlarged Mo-Mo and shortened Re–Re distances comparing to crystallographic data of **4**.

Fitting of the data obtained for $K_5[Re_3Mo_3Se_8(CN)_6]\cdot 11H_2O$ (**6**) salt reveals that, although only slightly smaller reliability factors, *the mer*-isomer model presents a set of final parameters more consistent than *fac*-one (see σ^2Mo-Mo Table S4 ; Figure S11) in agreement with the results of NMR spectroscopy. DFT optimized geometry for $[Re_3Mo_3Se_8(CN)_6]^{5-}$ discussed in our previous study [10] and geometry resulted from EXAFS fitting in present work were found to correlate similarly as it was found for $[Re_4Mo_2Se_8(CN)_6]^{4-}$ also comprising elongated Mo-Mo and shortened Re-Re distances (Table S6).

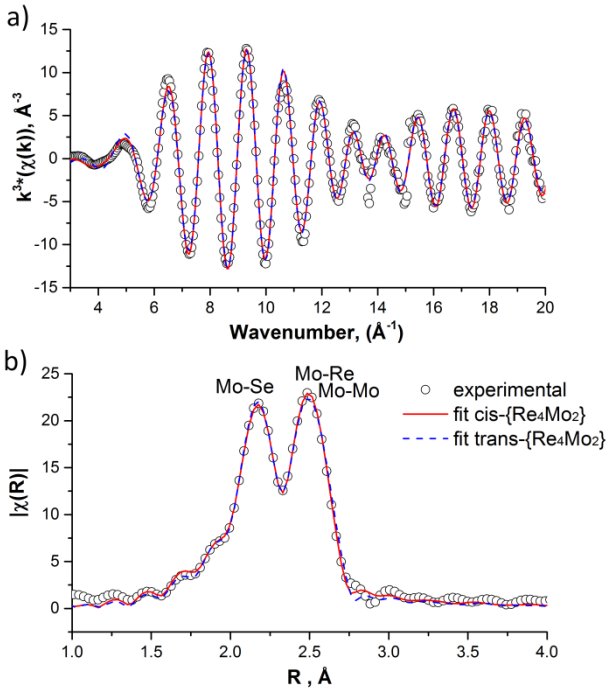


Figure 8. a) EXAFS measurements for the compound **4** (weighted by k^3) Mo K-edge, b) Fourier transform magnitudes. Model fits (fitting space – *k*) are reported as lines.

In this work we have carried out for the first time the detailed analysis of the structure of heterometallic cluster complexes $[Re_4Mo_2Se_8(CN)_6]^{n-}$ and $[Re_3Mo_3Se_8(CN)_6]^{n-}$. The data obtained by the use of X-Ray structural analysis and EXAFS agree well with the DFT calculations demonstrating significant distortion of metal octahedron upon electron removal, which however, keeps the average M–M distances at the similar values. ^{77}Se NMR measurements in solution have shown that the $[Re_3Mo_3Se_8(CN)_6]^{n-}$ anions contain the *mer*-$\{Re_3Mo_3Se_8\}$ isomer only while the $[Re_4Mo_2Se_8(CN)_6]^{n-}$ anions exist as the mixture of both *cis*- and *trans*- isomers of $\{Re_4Mo_2Se_8\}$ core. This investigation has become possible by the development of the synthetic method for separation and further characterization of $[Re_4Mo_2Se_8(CN)_6]^{n-}$ and $[Re_3Mo_3Se_8(CN)_6]^{n-}$ anions in individual phases from the solid solution $K_6[Re_{6-x}Mo_xSe_8(\mu\text{-}CN)(CN)_4]$ formed in high temperature synthesis due to the difference in redox behavior of anions with different Re/Mo ratio. Thus, it was shown that the substitution of metal atoms in cluster core and the variation in the ratio of metals is a powerful tool for changing the electronic structure and, as a consequence, the redox properties, UV-Vis spectra and color of octahedral cluster solutions and crystals. The discovered possibility to isolate these redox-active anions pave the way for the further engineering of cluster building blocks and new cluster materials with tailored physico-structural properties through ligand exchange reactions and formation of cluster solids by assembling of cluster building blocks via covalent and supramolecular interactions.

Acknowledgements

The research was supported by the Ministry of Science and Education of the Russian Federation. Authors are greatly acknowledged to French Synchrotron SOLEIL for the opportunity to use SAMBA XAS beamline. V. Muravieva thanks French Embassy for providing the scholarship for co-tutelle PhD program between France and Russia. The authors are acknowledged to International Associate Laboratory N° 1144 CLUSPOM between France and Russia. The authors thank the "Centre de Diffractométrie X" (CDIFX) of the Institute of Chemical Science of Rennes for single-crystal X-ray diffraction facilities. The authors also thank V. Dorcet for crystallographic data, Ph. Jéhan for mass-spectrometry and C. Orione for NMR.

Keywords: cluster compounds • heterometallic complexes • EXAFS • structure • electronic structure

[1] a) H. D. Yoo, I. Shterenberg, Y. Gofer, G. Gershinsky, N. Pour, D. Aurbach, *Energy Environ. Sci.* **2013**, *6*, 2265-2279; b) L. Mei, J. T. Xu, Z. X. Wei, H. K. Liu, Y. T. Li, J. M. Ma, S. X. Dou, *Small* **2017**, *13*.
[2] S. Cordier, Y. Molard, K. A. Brylev, Y. V. Mironov, F. Grasset, B. Fabre, N. G. Naumov, *J. Clust. Sci.* **2014**, *26*, 53-81.
[3] A. A. Krasilnikova, M. A. Shestopalov, K. A. Brylev, I. A. Kirilova, O. P. Khripko, K. E. Zubareva, Y. I. Khripko, V. T. Podorognaya, L. V. Shestopalova, V. E. Fedorov, Y. V. Mironov, *J. Inorg. Biochem.* **2015**, *144*, 13-17.
[4] J.-C. P. Gabriel, K. Boubekeur, S. Uriel, P. Batail, *Chem. Rev.* **2001**, *101*, 2037-2066.
[5] a) V. I. Baranovski, D. V. Korolkov, *Polyhedron* **2004**, *23*, 1519-1526; b) A. Deluzet, H. Duclusaud, P. Sautet, S. A. Borshch, *Inorg. Chem.* **2002**, *41*, 2537-2542; c) T. G. Gray, *Chem. - Eur. J.* **2009**, *15*, 2581-2593; d) T. G. Gray, C. M. Rudzinski, E. E. Meyer, R. H. Holm, D. G. Nocera, *J. Am. Chem. Soc.* **2003**, *125*, 4755-4770.
[6] a) A. Pinkard, A. M. Champsaur, X. Roy, *Account. Chem. Res.* **2018**, *51*, 919-929; b) E. V. Alexandrov, A. V. Virovets, V. A. Blatov, E. V. Peresypkina, *Chem. Rev.* **2015**, *115*, 12286-12319.
[7] A. Perrin, M. Sergent, O. Fischer, *Mater. Res. Bull.* **1978**, *13*, 259-264.
[8] a) A. Perrin, R. Chevrel, M. Sergent, O. Fischer, *J. Solid State Chem.* **1980**, *33*, 43-47; b) W. Honle, H. D. Flack, K. Yvon, *J. Solid State Chem.* **1983**, *49*, 157-165; c) F. J. Berry, C. D. Gibbs, *Dalton Trans.* **1991**, 57-59; d) F. J. Berry, C. D. Gibbs, C. Greaves, *J. Solid State Chem.* **1991**, *92*, 148-153.
[9] N. G. Naumov, K. A. Brylev, Y. V. Mironov, A. V. Virovets, D. Fenske, V. E. Fedorov, *Polyhedron* **2004**, *23*, 599-603.

Accepted Manuscript

[10] V. K. Muravieva, Y. M. Gayfulin, M. R. Ryzhikov, I. N. Novozhilov, D. G. Samsonenko, D. A. Piryazev, V. V. Yanshole, N. G. Naumov, *Dalton Trans.* **2018**, *47*, 3366-3377.

[11] C. Magliocchi, X. Xie, T. Hughbanks, *Inorg. Chem.* **2004**, *43*, 1902-1911.

Accepted Manuscript

10.1002/chem.201903321

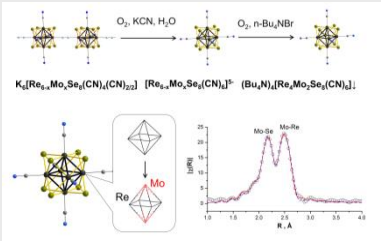
WILEY-VCH

Entry for the Table of Contents (Please choose one layout)

Layout 1:

COMMUNICATION

Excision reaction of polymeric phase $K_6[Re_{3.6}Mo_{2.4}Se_8(m\text{-}CN)(CN)_4]$ and selective oxidation afford the individual heterometallic redox-active $[Re_4Mo_2Se_8(CN)_6]^{n-}$ and $[Re_3Mo_3Se_8(CN)_6]^{n-}$ cyanoclusters. Electron deficient anions demonstrate significant metal core distortion determined by EXAFS and DFT calculations.



*V.K. Muravieva, Y.M. Gayfulin, C. Prestipino, P. Lemoine, M.R. Ryzhikov, V.V. Yanshole, S. Cordier, N.G. Naumov**

Page No. – Page No.

Tailoring heterometallic cluster functional building blocks: synthesis, separation, structural and DFT studies of $[Re_{6-x}Mo_xSe_8(CN)_6]^{n-}$

Layout 2:

COMMUNICATION

((Insert TOC Graphic here))

*Author(s), Corresponding Author(s)**

Page No. – Page No.

Title

Text for Table of Contents

Accepted Manuscript